BioOne COMPLETE

Constitutive Activation of Beta-Catenin in Uterine Stroma and Smooth Muscle Leads to the Development of Mesenchymal Tumors in Mice 1

Authors: Tanwar, Pradeep S., Lee, Ho-Joon, Zhang, LiHua, Zukerberg, Lawrence R., Taketo, Makoto M., et al.

Source: Biology of Reproduction, 81(3) : 545-552

Published By: Society for the Study of Reproduction

URL: https://doi.org/10.1095/biolreprod.108.075648

BioOne Complete (complete.BioOne.org) is a full-text database of 200 subscribed and open-access titles in the biological, ecological, and environmental sciences published by nonprofit societies, associations, museums, institutions, and presses.

Your use of this PDF, the BioOne Complete website, and all posted and associated content indicates your acceptance of BioOne's Terms of Use, available at www.bioone.org/terms-of-use.

Usage of BioOne Complete content is strictly limited to personal, educational, and non - commercial use. Commercial inquiries or rights and permissions requests should be directed to the individual publisher as copyright holder.

BioOne sees sustainable scholarly publishing as an inherently collaborative enterprise connecting authors, nonprofit publishers, academic institutions, research libraries, and research funders in the common goal of maximizing access to critical research.

Downloaded From: https://bioone.org/journals/Biology-of-Reproduction on 28 Mar 2024
Terms of Use: https://bioone.org/terms-of-use

BIOLOGY OF REPRODUCTION **81,** 545–552 (2009)
Published online before print 29 April 2009.
DOI 10.1095/biolreprod.108.075648

Constitutive Activation of Beta-Catenin in Uterine Stroma and Smooth Muscle Leads to the Development of Mesenchymal Tumors in Mice[1]

Pradeep S. Tanwar,[3] Ho-Joon Lee,[3] LiHua Zhang,[3] Lawrence R. Zukerberg,[4] Makoto M. Taketo,[5] Bo R. Rueda,[3] and Jose M. Teixeira[2,3]

Vincent Center for Reproductive Biology, Vincent Obstetrics and Gynecology Services,[3] and Department of Pathology,[4] Massachusetts General Hospital and Harvard Medical School, Boston, Massachusetts
Department of Pharmacology,[5] Graduate School of Medicine, Kyoto University, Japan

ABSTRACT

Leiomyomas and other mesenchymally derived tumors are the most common neoplasms of the female reproductive tract. Presently, very little is known about the etiology and progression of these tumors, which are the primary indication for hysterectomies. Dysregulated WNT signaling through beta-catenin is a well-established mechanism for tumorigenesis. We have developed a mouse model that expresses constitutively activated beta-catenin in uterine mesenchyme driven by the expression of Cre recombinase knocked into the Müllerian-inhibiting substance type II receptor promoter locus to investigate its effects on uterine endometrial stroma and myometrium. These mice show myometrial hyperplasia and develop mesenchymal tumors with 100% penetrance that exhibit histological and molecular characteristics of human leiomyomas and endometrial stromal sarcomas. By immunohistochemistry, we also show that both transforming growth factor beta and the mammalian target of rapamycin are induced by constitutive activation of beta-catenin. The prevalence of the tumors was greater in multiparous mice, suggesting that their development may be a hormonally driven process or that changes in uterine morphology during pregnancy and after parturition induce injury and repair mechanisms that stimulate tumorigenesis from stem/progenitor cells, which normally do not express constitutively activated beta-catenin. Additionally, adenomyosis and endometrial gland hyperplasia were occasionally observed in some mice. These results show evidence suggesting that dysregulated, stromal, and myometrial WNT/beta-catenin signaling has pleiotropic effects on uterine function and tumorigenesis.

adenomyosis, beta-catenin, developmental biology, endometrial stromal sarcoma, hypertrophic scarring, leiomyoma, signal transduction, uterine fibroids, uterus, WNT signaling

INTRODUCTION

Mesenchymal uterine tumors are the most common neoplasms found in the human female reproductive tract. The vast majority of these tumors are uterine leiomyomas (uterine fibroids), which are benign lesions that form in the myometrium of an estimated 25%–50% of American women. Uterine leiomyomas are clonal in origin and hormone responsive [1]. Patients may have a single uterine fibroid, but many have multiple fibroids, and they can be located anywhere in myometrial tissue. These tumors are commonly associated with severe pelvic discomfort during menstruation (dysmenorrhea), heavy menstrual bleeding (menorrhagia), infertility, abortion, ascites, and polycythemia. On the basis of their location in the uterus, fibroids are subdivided into three broad categories: subserosal, submucosal, and intramural. The size of the fibroids can vary greatly from microscopic to tumors weighing more than 1 kg, are often associated with significant morbidities, and are the leading cause of hysterectomies [2]. Other uterine tumors such as leiomyosarcomas, endometrial stromal sarcomas (ESSs), perivascular epitheliod cell tumors (PEComa), and adenocarcinomas are less common but still pose a significant burden on a women's health and are often fatal. The etiology of any of these mesenchymal tumors is largely unknown.

One of the major mechanisms of neoplastic transformation is dysregulated β-catenin signaling. β-Catenin is the core component of the canonical wingless-type MMTV integration site family member (WNT) signaling pathway whose activation leads to the translocation of β-catenin from the cytoplasm to the nucleus and transcription of targeted genes [3]. The role of WNT signaling in carcinogenesis in other tissues is well documented [4], but evidence for its contribution to mesenchymal uterine tumor development has been limited [5–7]. WNT signaling is indispensible for normal uterine development from the primordial Müllerian duct [8–10], and there is accumulating evidence to support a role for WNT signaling in postnatal uterine functions, including implantation [11], decidualization [12, 13], and perhaps remodeling after parturition.

We have been investigating β-catenin signaling in uterine development and function using a mouse Cre recombinase model system [14, 15] that exploits the uterine mesenchyme-specific expression of the Müllerian inhibiting substance type II receptor, which is also known as anti-Müllerian hormone 2 (AMHR2). We have shown that conditional deletion of β-catenin in uterine mesenchyme leads to progressive cell fate change from myogenesis to an adipogenic lineage [15]. The aim of the present study was to investigate the role of β-catenin in uterine development further by expressing a constitutively activated form of β-catenin in uterine mesenchyme driven by *Amhr2*-Cre. When $Amhr2^{tm3(cre)Bhr}$ (*Amhr2*-Cre) mice are crossed with $Ctnnb1^{tm1Mmt}$ mice [16], *Amhr2*-driven Cre recombinase, which is expressed in ovary, oviduct, and uterus, deletes exon3 and leads to formation of a stable form of β-catenin in *Amhr2*-Cre-expressing cells and in their progeny.

[1]Supported by a grant from the National Institute of Child Health and Human Development, HD052701, to J.M.T.
[2]Correspondence: Jose M. Teixeira, Vincent Center of Reproductive Biology/Thier 913 Massachusetts General Hospital and Harvard Medical School, 55 Fruit St., Boston, MA 02114. FAX: 617 726 0561; e-mail: teixeira@helix.mgh.harvard.edu

Received: 15 December 2008.
First decision: 12 January 2009.
Accepted: 9 April 2009.
© 2009 by the Society for the Study of Reproduction, Inc.
This is an Open Access article, freely available through *Biology of Reproduction's* Authors' Choice option.
eISSN: 1259-7268 http://www.biolreprod.org
ISSN: 0006-3363

Downloaded From: https://bioone.org/journals/Biology-of-Reproduction on 28 Mar 2024
Terms of Use: https://bioone.org/terms-of-use

TABLE 1. Oocyte and embryo analysis in *Amhr2*$^{tm3(cre)Bhr}$/+; *Ctnnb1*^{tm1Mmt}/+ mice.*

Stage	Control	*Amhr2*$^{tm3(cre)Bhr}$/+; *Ctnnb1*^{tm1Mmt}/+
Oocytes		
MII	27.7 ± 9.1 (75%)	20.0 ± 7.0 (77%)
GVBD	4.0 ± 2.7 (11%)	2.0 ± 0 (8%)
GV	0 (0%)	0.3 (1%)
Atretic	4.7 ± 2.5 (13%)	3.7 ± 1.5 (14%)
Total	36.3 ± 7.7	26.0 ± 7.8
Embryos†		
Four-cell to morula	6 ± 2 (21%)	3 ± 1 (19%)
Early blastocyst	5.3 ± 2 (19%)	3.7 ± 1.2 (24%)
Expanded blastocyst	16.7 ± 3.8 (60%)	9 ± 2.0 (57%)
Total	28 ± 2.0	15.7 ± 3.2

* n = 3; mean ± SD (% of total).
† Two out of six oviducts were blocked in mutant mice.

This form of β-catenin is resistant to phosphorylation by the adenomatosis polyposis coli complex and its subsequent degradation. We show that dysregulated WNT signaling in the uteri of these mice causes mesenchymal tumorigenesis in all mice examined and occasional adenomyosis, with probable indirect stromal support for the induction of adenocarcinoma.

MATERIALS AND METHODS

Mouse Husbandry

The mice used in this study were housed under standard animal housing conditions. All protocols involving animal experimentation were approved by the Institutional Animal Care and Use Committee at Massachusetts General Hospital. Mice were maintained on C57BL/6;129/SvEv mixed genetic background. *Amhr2*$^{tm3(cre)Bhr}$ (*Amhr2*-Cre) mice [17] (Dr. Richard Behringer, M.D. Anderson, Houston, TX) were mated with *Ctnnb1*$^{tm1Mmt/tm1Mmt}$ [16] to generate *Amhr2*$^{tm3(cre)Bhr}$/+;*Ctnnb1*^{tm1Mmt}/+ mice. The DNA from tail biopsies was used to genotype mice using the standard PCR protocols. The uterus collected from *Amhr2*$^{tm3(cre)Bhr}$/+;*Ctnnb1*^{tm1Mmt}/+ and control mice were photographed by using a Nikon SMZ1500 microscope with an attached Spot camera (Diagnostic Instruments, Sterling Heights, MI).

Oocyte and Blastocyst Collection and Assessment

The 6- to 7-wk-old mutant and control mice were superovulated with i.p. injections of 7.5 IU equine chorionic gonadotropin (eCG; Sigma Chemical Co., St. Louis, MO) followed by 7.5 IU human chorionic gonadotropin (hCG; Sigma) after 48 h. Fourteen hours after hCG injection, females were euthanized, and their oviducts were removed. The cumulus-oocyte complexes were released from the ampullary region of each oviduct by puncturing the oviduct. Cumulus cells were removed by exposure to 80 IU/ml hyaluronidase (Irvine Scientific, Santa Ana, CA) in Hepes buffer and washed out with human tubal fluid (HTF; Irvine Scientific) with 10% fetal bovine serum (FBS). Isolated oocytes were transferred into HTF media with 10% FBS and assessed by morphology. Oocytes were classified into four groups as mature, germinal vesicle break down, immature, and atretic. For blastocysts, the 6- to 7-wk-old mutant and control mice were superovulated with 7.5 IU eCG and 7.5 IU hCG as above then mated with wild-type males. Mice were euthanized at 3.5 days after mating, and uteri were removed. Blastocysts were flushed from the uteri and transferred into HTF media with 10% FBS and assessed by morphology. Blastocysts were classified as 4-cell to morula, expanded blastocyst, and early blastocyst.

Histology

Human myometrial and fibroid samples were collected using Institutional Review Board approved protocols. Murine uteri and human samples were fixed by immersion in 4% paraformaldehyde for 10–12 h and then transferred to 70% ethanol until processing. The fixed tissues were dehydrated in a graded ethanol series, cleared in xylene, and embedded in paraffin wax. Embedded tissue samples were sectioned at 5-μm thickness and mounted on slides. Hematoxylin and eosin (H&E) staining was performed using standard histological techniques. Photomicrographs of nontumorous myometria (n = 3 mice for each group) were measured to determine the ratio of the width of myometria to total uterine width.

In Situ Hybridization

Analyses for *Amhr2* mRNA are described in a detail in a previous study [14, 15]. Briefly, urogenital ridges were collected from timed pregnant dams and at Embryonic Day 13.5 (E13.5) and fixed overnight at 4°C in 4% paraformaldehyde. Tissues were pretreated with protease prior to overnight hybridization with either *Amhr2* full-length [18] digoxigenin-labeled antisense riboprobes in 50% formamide hybridization solution at 70°C. The resultant hybrids were detected with alkaline phosphatase-conjugated antidigoxigenin antibodies and BM purple colorimetric solution (Roche Molecular Biochemicals, Indianapolis, IN).

Immunofluorescence

Serial sections of tissues were deparaffinized with xylene and rehydrated with graded series of ethanol (absolute, 95%, 80%, and 50%, respectively, and distilled water), followed by two washes of 5 min each in PBS containing 0.05% Tween 20 (PBS-T). After a wash with PBS-T, antigen retrieval was performed by boiling the tissue sections in 0.01 M citrate buffer (pH 6) for 20 min. Sections were then washed for 5 min in PBS-T and blocked at room temperature for 1 h by using 2% normal donkey or goat serum, 2% bovine serum albumin, and 0.1% triton-X in PBS. Tissue sections were then incubated in a humidified chamber overnight at 4°C with primary antibody. Sections were subsequently washed with PBS-T, incubated at room temperature for 1 h with secondary antibody, then counterstained with 4′,6′-diamidino-2-phenylindole (DAPI). Images were photographed using a microscope (Nikon Eclipse TE 2000-S; Micro Video Instruments, Avon, MA) equipped with a Spot digital camera. DAPI-stained nuclei and phospho-histone H3 (pH3)-positive cells from sections of three different lesions were counted with the nucleus-counting analysis plugin of Image J software (v1.37; NIH, Bethesda, MD) after setting a black and white threshold at 27–30 in Photoshop (v10; Adobe Systems Inc., San Jose, CA).

Antibodies

Following are the primary and secondary antibodies used in this study: anti-β-catenin (1:250; BD Transduction Laboratories, San Jose, CA); anti-KIT (1:200; R&D Systems, Minneapolis, MN); anti-TGFB3 (1:200; Abcam, Cambridge, MA); anti-HMGA2 and anti-PECAM1 (1:200; Santa Cruz Biotechnology, Santa Cruz, CA); anti-vimentin (1:200; Santa Cruz Biotechnology); anti-Ecadherin (1:100; Santa Cruz Biotechnology); anti-pH3 (1:200; BD Transduction Laboratories); anti-CD11B (1:100; eBiosciences, San Diego, CA); anti-CD140B (1:200; Ebiosciences); anti-ACTA2, CY3-conjugated (Sigma); anti- PCNA (ready to use; Zymed, San Francisco, CA); anti-FRAP1 (1:200; Cell Signaling, Danvers, MA); AlexaFluor secondary antibodies (1:500; Invitrogen, Carlsbad, CA); and biotinylated donkey anti-mouse or anti-rabbit antibody $F(ab)_2$ (1:1000; Jackson ImmunoResearch Laboratories, West Grove, PA).

RESULTS

A previous study has shown that despite normal ovarian functions, *Amhr2*$^{tm3(cre)Bhr}$/+;*Ctnnb1*^{tm1Mmt}/+ mutant mice were subfertile [19]. In our study we also observed that *Amhr2*$^{tm3(cre)Bhr}$/+;*Ctnnb1*^{tm1Mmt}/+ mice have smaller litters in younger mice despite their having histologically normal ovaries (data not shown). Further analyses showed that neither oocyte nor 3-day-old embryo quality appeared to be significantly affected by constitutive activation of β-catenin in the ovary (Table 1). However, fewer oocytes and embryos were collected from the mutant uteri (Table 1), which is likely in part because of structural blockage we observed in some of the mutant oviducts (data not shown). We next analyzed the uteri to determine if the subfertility in mutant mice might also be due, in part, to defective development in mutant uteri. Below we show evidence that expression of constitutively activated β-catenin in mouse uteri results in the appearance of two types of mesenchymal tumors that resemble human leiomyomas and ESSs (Table 2).

Leiomyoma-Like Lesions

Amhr2$^{tm3(cre)Bhr}$/+;*Ctnnb1*^{tm1Mmt}/+ mutant and *Amhr2*$^{tm3(cre)Bhr}$/+ or *Ctnnb1*^{tm1Mmt}/+ control mice were

Downloaded From: https://bioone.org/journals/Biology-of-Reproduction on 28 Mar 2024
Terms of Use: https://bioone.org/terms-of-use

TABLE 2. Incidence of mesenchymal tumors in *Amhr2*$^{tm3(cre)Bhr}$/+;*Ctnnb1*^{tm1Mmt}/+ mice.

Age of mice	Phenotype observed	No. of animals examined per phenotype	No. of animals with tumorous phenotype (%)
<6 wk (nulliparous)	Smooth muscle tumor and hyperplasia	5	5 (100)
	Endometrial stromal sarcoma-like lesions	5	5 (100)
≥8 wk (nulliparous)	Smooth muscle tumor and hyperplasia	5	5 (100)
	Endometrial stromal sarcoma-like lesions	5	5 (100)
≥12 wk (multiparous)	Smooth muscle tumor and hyperplasia	14	14 (100)
	Endometrial stromal sarcoma-like lesions	14	14 (100)
	Adenomyosis	14	2 (14.28)

examined for phenotypic analysis. Initial gross examination of adult nulliparous mutant uteri occasionally showed hemorrhagic areas (data not shown) along both horns and an extraneous layer of tissue with protruding nodules at the anti-mesometrial side of the uteri (Fig. 1A). Examination of mutant uteri from multiparous mice revealed the presence of large tumorous growths and consistent multiple hemorrhagic sites on the surface of the uteri (Fig. 1B). No abnormalities were detected in the uteri collected from control mice (Fig. 1C). Histological examination of noncycling 4-wk-old uteri showed that the nodules observed on the surface of uteri appear to originate from the longitudinal myometrial layer of the uterus (shown with a red arrowhead in Fig. 1D). We also observed a small area of dysplasia (shown with a black arrowhead and outlined in white) in the mutant uteri, which otherwise appear similar to controls (Fig. 1E), suggesting that tumorigenesis starts before the mice begin estrous cycling. Staining of the mutant and control uteri for α-smooth muscle actin (ACTA2) shows that the polyps are derived from the myometrium and that there was expansion of the myometrium in the mutants (Fig. 1, F and G). The ratio of the width of ACTA2-positive myometrium to total uterine width in the mutant (0.45 ± 0.04, $n = 3$) was significantly higher ($P = 0.009$) than that of control uteri (0.22 ± 0.03, $n = 3$) suggesting smooth muscle hyperplasia. Normal WNT signaling is highly active at the coelomic epithelium of the Müllerian duct [20]. The nodules we observe in the mutant mice may be the result of constitutively activated β-catenin on the coelomic epithelium and adjacent mesenchyme of the presumptive anti-mesometrial side of the E13.5 urogenital ridge where *Amhr2* is highly expressed (Fig. 1H).

In mutant mouse uteri, we observed dysplastic lesions in myometria with 100% penetrance that appeared to increase in size and number with age and parity (Fig. 2, A and B, and Table 2). The mutant murine tumors were composed of plump spindle cells surrounded by an extracellular matrix that formed fascicles (Fig. 2C) that are remarkably similar to those typically found in human uterine leiomyomas [2] (Fig. 2D). The largest tumors were often necrotic with hemorrhagia and fibrosis (data not shown). The murine smooth muscle tumors are ACTA2-positive (Fig. 2, E–G), which is also characteristic of human uterine leiomyomas (Fig. 2H). Typically, human uterine leiomyomas are very slow-dividing tumors and are usually present with a low proliferative index (0–2 mitoses per 10 high power field) [21]. We analyzed proliferation in the uterine smooth muscle tumors observed in mutant mice by performing pH3 expression analysis and found few pH3-positive cells (5–6 per high-powered filed or 2.4 ± 0.2/1000 cells) in these tumors, whereas pH3 expression was high in luminal epithelium (LE; Fig. 2, I and J). Proliferating cell nuclear antigen (PCNA) expression was also analyzed with similar results (data not shown). These data suggest that, similar to human uterine leiomyomas and unlike most other more aggressive tumors, these mouse uterine smooth muscle tumors also have a low mitotic activity. Another characteristic of many human uterine leiomyomas is that leiomyomas express higher levels of TGFB, particularly TGFB3, than the surrounding myometrium [22–26]. Analysis of TGFB3 in the uteri of mutant mice showed much higher levels of expression by immunohistochemistry in the epithelium and endometrial stroma, as well as in the central areas of the leiomyoma-like lesions, than in surrounding areas and the remaining myometrium and at levels consistent with those observed in human leiomyoma (Fig. 2, K and L). Together with the appearance of polyps shown above, these results suggest that constitutively

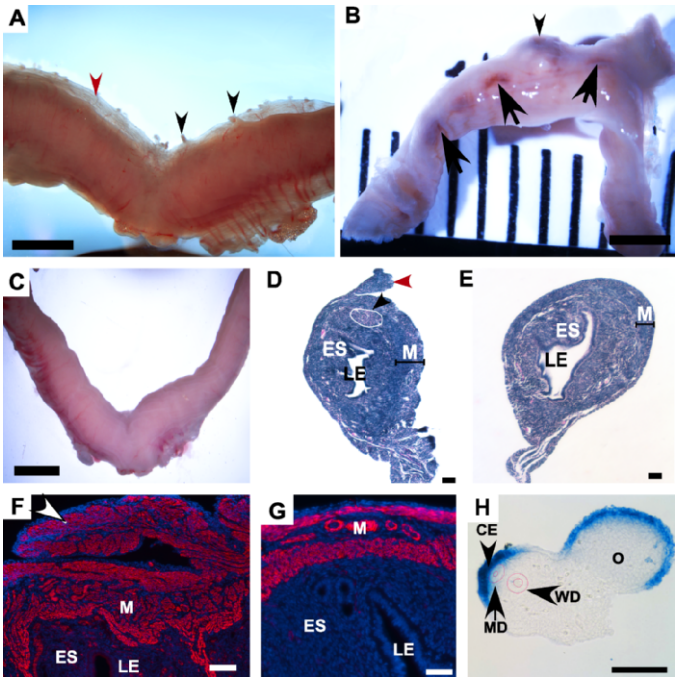


FIG. 1. Constitutive activation of β-catenin in uterine mesenchyme. **A**) Gross uterus from *Amhr2*$^{tm3(cre)Bhr}$;*Ctnnb1*^{tm1Mmt}/+ nulliparous mouse showing abnormal growth (black and red arrowheads) on the anti-mesometrial side of the uterus. Nodules were also observed on the surface of the uterus (black arrowheads). **B**) Gross uterus from multiparous adult *Amhr2*$^{tm3(cre)Bhr}$;*Ctnnb1*^{tm1Mmt}/+ mouse showing tumorous growth (black arrowhead) and multiple hemorrhagic sites (black arrows). **C**) Normal uterus from a control *Amhr2*$^{tm3(cre)Bhr}$/+ mouse. H&E-stained section of 4-wk-old mutant uterus (**D**) showing polyp-like growth protruding from the myometrium on the anti-mesometrial surface of the uterus (red arrowhead) and ESS-like lesions in the endometrial stroma (black arrowhead) and control uterus (**E**). ACTA2-immunostained longitudinal section of a nulliparous mutant uterus (**F**) with positively stained polyps (white arrowhead) and control (**G**). **H**) In situ hybridization in the E13.5 urogenital ridge shows that the *Amhr2* mRNA is expressed in the coelomic epithelium and subjacent mesenchyme of the Müllerian duct (outlined in red with the Wolffian duct). CE, coelomic epithelium; MD, Müllerian duct; WD, Wolffian duct; O, ovary; LE, luminal epithelium; ES, endometrial stroma; M, myometrium. Bars = 2 mm (**A**–**C**), 50 μm (**D**–**H**).

Downloaded From: https://bioone.org/journals/Biology-of-Reproduction on 28 Mar 2024
Terms of Use: https://bioone.org/terms-of-use

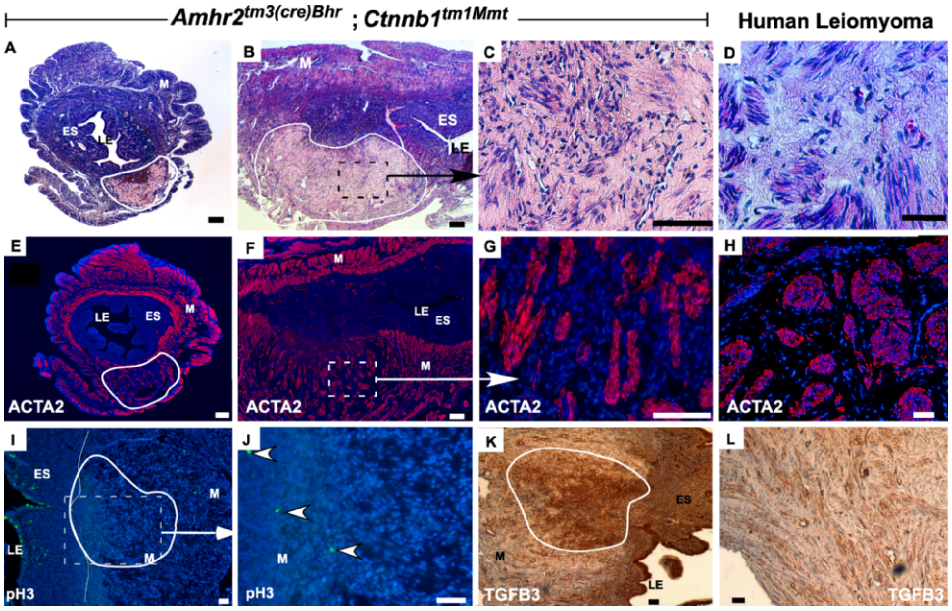


FIG. 2. *Amhr2*$^{tm3(cre)Bhr}$;*Ctnnb1*^{tm1Mmt}/+ mutant mice develop smooth muscle tumors of uterine myometrium. H&E-stained cross (**A**) and longitudinal (**B**) sections of mutant uteri showing the smooth muscle tumor (outlined with white line) in the myometrium. H&E-stained section of mutant uterus (**C**) at higher magnification showing tumorous growth (outlined in white in **B**) and human leiomyoma (**D**). Serial sections of mutant uteri in **A** and **B** are shown stained with ACTA2 antibody in **E** and **F**. **G**) Higher magnification image of neoplastic area from **F** showing that most of the tumorous cells are positive for ACTA2. **H**) Representative section of a human uterine smooth muscle tumor showing the typical staining pattern with the ACTA2 antibody. Phosphohistone staining of tumor area in a mutant uterus is shown in **I** and at higher magnification with white arrows in **J**. **K** and **L**) TGFB3 immunostaining in the central area of a mutant smooth muscle tumor and a human leiomyoma, respectively. Nuclei are stained with DAPI or hematoxylin. LE, luminal epithelium; ES, endometrial stroma; M, myometrium. Bar = 50 μm.

activated β-catenin induces smooth muscle hyperplasia, which can then lead to smooth muscle tumor development.

The oncogenic serine/threonine kinase, mammalian Target of Rapamycin (FRAP1), which lies downstream of the PI3K signaling pathway and is a master regulator of cell proliferation [27], is up-regulated in the Eker rat leiomyoma model because of a mutation in tuberous sclerosis 2 (*Tsc2*) [28]. We assayed whether FRAP1 is also induced in these tumors by constitutively activated β-catenin using immunohistochemistry (Fig. 3). In the mutant with CA β-catenin, FRAP1 appears highly expressed in the central portion of the leiomyoma-like lesion, with little expression observed in the surrounding hypocellular areas (Fig. 3A). Relatively strong FRAP1 expression was also observed in both the circular and longitudinal myometrial layers (Fig. 3B). In the normal myometrium of control mice, FRAP1 expression appears to be limited to the endothelial cells or pericytes (Fig. 3, C and D).

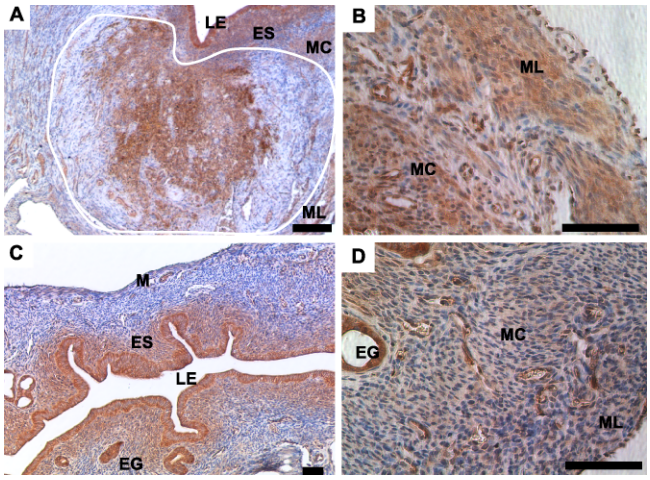


FIG. 3. FRAP1 expression in *Amhr2*$^{tm3(cre)Bhr}$;*Ctnnb1*^{tm1Mmt} uteri. **A**) FRAP1 expression was detected by immunohistochemistry at high levels in the central areas of a leiomyoma (outlined in white) in a mutant uterus, the epithelial cells, the ES as well as in the circular myometrial layer (MC) and longitudinal myometrial layer (ML). **B**) A higher magnification view of FRAP1 expression in the MC and ML of a mutant mouse. **C**) In control uteri, strong FRAP1 expression is found in the EG, LE, and ES. **D**) Expression in the control myometrium appears limited to the endothelial cells. LE, luminal epithelium; ES, endometrial stroma; M, myometrium; EG, endometrial glands. Bars = 50 μm (**A** and **C**), 100 μm (**B** and **D**).

ESS-Like Lesions

In addition to uterine smooth muscle tumors, *Amhr2*$^{tm3(cre)Bhr}$/+;*Ctnnb1*^{tm1Mmt}/+ mutants also developed ESS-like neoplastic lesions that were restricted to the endometrial stroma (ES; Fig. 4A). These lesions were ACTA2-negative (Fig. 4B), which we used as a marker to distinguish between ESS and ACTA2-positive leiomyomas. These tumors expressed high levels of nuclear β-catenin, indicating their origin from *Amhr2*-Cre-expressing mesenchymal cells (Fig. 4C). As expected, only membranous β-catenin is detected in LE and endometrial glands (EG) of both mutant (Fig. 4C) and control uterus (Fig. 4D), since *Amhr2* is not expressed in these cells [15]. Some cells at the junction of the longitudinal and circular smooth muscle layers also expressed nuclear β-catenin (Fig. 4D). The ESS-like tumors expressed vimentin, a mesenchymal marker, suggesting the mesenchymal origin of these tumors (Fig. 4E). Consistent with a previous study [29], vimentin is also expressed in ES and blood vessels of both the mutant and control uteri (Fig. 4F).

Further analysis of the ESS-like neoplastic lesions with various markers used in the diagnosis of human tumors was performed to determine how well the murine tumors compare.

Downloaded From: https://bioone.org/journals/Biology-of-Reproduction on 28 Mar 2024
Terms of Use: https://bioone.org/terms-of-use

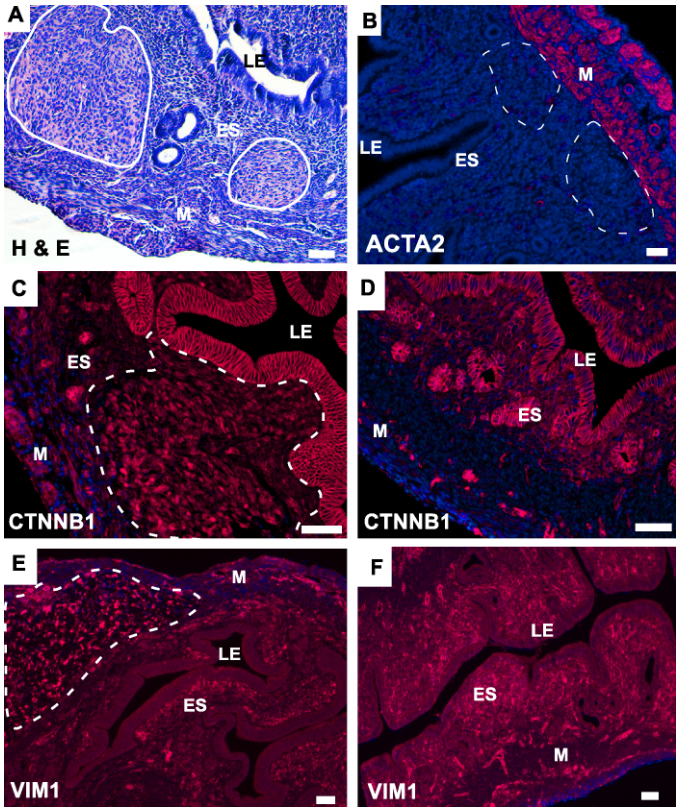


FIG. 4. Constitutive activation of β-catenin causes development of ESS-like tumors in mouse uteri. **A**) H&E-stained section of mutant uterus. Neoplastic lesions are seen in endometrial stroma (outlined in white). **B**) ESS-like neoplastic growths are ACTA2-negative. The dotted lines indicate the location of ESS lesions detected on a serial section by H&E. **C**) Both cytoplasmic and nuclear staining for β-catenin were observed in tumorous lesions (outlined by white dotted line) and normal-looking myometrium of mutant uterus. Membranous staining for β-catenin is present in the LE and EG of mutant uteri and in control mice (**D**). **E**) The ESS-like tumors were vimentin-positive but in a pattern that was different from that observed normally in stromal areas of mutants and in control stroma (**F**). Nuclei are stained with DAPI. LE, luminal epithelium; ES, endometrial stroma; M, myometrium. Bar = 50 μm.

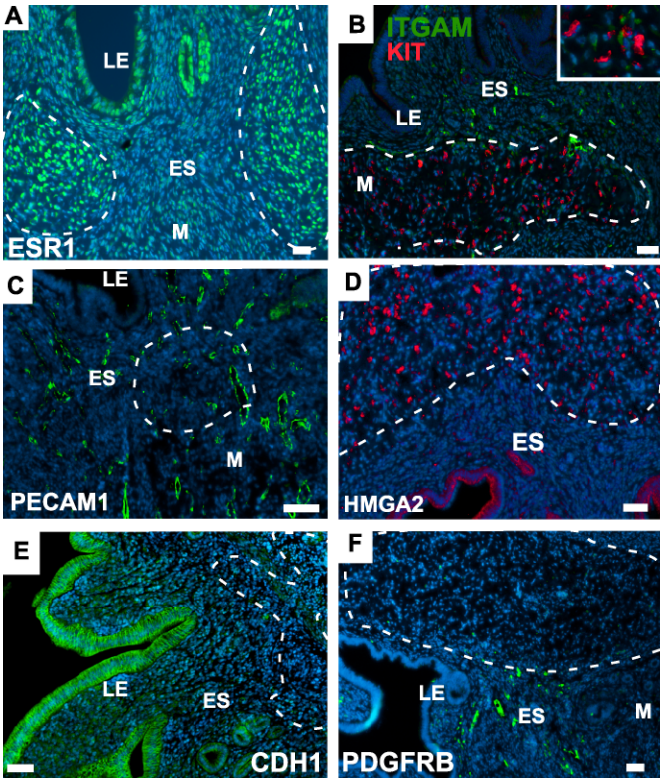


FIG. 5. Sections of the mutant uteri with ESS-like tumors, outlined in a white dashed line in all the panels, were analyzed by immunofluorescence for various markers. The tumors were ESR1-positive (**A**), KIT-positive (**B**), and were negative for the pan-hematopoietic marker ITGAM (CD11B) and the endothelial marker PECAM1 (**C**). The ESS-like lesions were also positive for HMGA2 (**D**), and negative for E-cadherin (CDH1) (**E**) and PDGFRB (CD140B) (**F**). Nuclei are shown stained with DAPI. LE, Luminal epithelium; ES, Endometrial stroma; M, Myometrium. Bars = 50 μm.

The ESS-like neoplastic growths observed in mutant uterus are strongly estrogen receptor alpha (ESR1) positive (Fig. 5A), suggesting that these tumors can be responsive to changes in the levels of estrogen. KIT (CD117) is the tyrosine kinase receptor for the stem cell factor that has been shown to be expressed at relatively high levels in uterine sarcomas and mesenchyme-derived tumors of the uterus [30, 31]. We also find high levels of KIT expression in the ESS-like tumors (Fig. 5B). Co-staining with ITGAM (CD11B), a monocyte/macrophage cell marker, was performed to ensure that the KIT^{+} cells were not hematopoietic cells that had infiltrated the lesion. In the rest of the endometrial stroma, KIT is only expressed in a few cells, probably of hematopoietic origin. In addition, these tumorous lesions do not express PECAM1, an endothelial cell marker, except for the endothelial cells of blood vessels present inside the tumorous area (Fig. 5C). HMGA2 is a member of the high mobility group (HMG) of proteins. The disruption and misexpression of HMGA2 has been reported in various benign mesenchymal tumors such as lipomas, uterine leiomyomas, endometrial polyps, and salivary gland adenomas [32, 33]. In mutant uteri, we detected very high expression of HMGA2 in ESS-like tumor lesions compared with the normal adjacent tissue (Fig. 5D). Although E-cadherin, an epithelial cell marker, and PDGFRB (CD140B), a fibroblast marker, were expressed in normal LE and a few scattered cells of ES and myometrium, respectively, they were not expressed in ESS-like tumors of mutant uteri (Fig. 5, E and F). These results suggest that the ESS-like tumors in *Amhr2*$^{tm3(cre)Bhr}$/+;*Ctnnb1*^{tm1Mmt}/+ mice strongly resemble ESS tumors found in human uteri both by histology and by marker profile.

Adenomyosis

The mutations in phosphorylation sites on exon 3 of the β-catenin gene have been shown to occur in various tumors [34, 35]. In humans, 38% of cases of endometrial carcinoma show nuclear and/or cytoplasmic accumulation of β-catenin, suggesting that β-catenin plays an important role in the development of this disease [36]. In the present study, we observed hyperplasia and pseudostratification of epithelia of EGs in 14% of the mutant uteri (Table 2). We also observed aberrant EGs in the myometrium of the mutant uteri (Fig. 6A). The colocalization of ACTA2 and E-cadherin further confirms the presence of EGs in the myometrial layer of the mutant uteri (Fig. 6B). These phenotypic changes observed in EGs were surprising because *Amhr2*-Cre is only expressed in the stromal and myometrial compartments of the uterus [15], and the activation of β-catenin only occurred in these two compartments (Fig. 2). However, correctly functioning uterine stroma is required for normal adenogenesis [10], and our previous study has shown that conditional deletion of β-catenin from ES and the myometrium leads to fewer EGs [15]. Collectively, our

Downloaded From: https://bioone.org/journals/Biology-of-Reproduction on 28 Mar 2024
Terms of Use: https://bioone.org/terms-of-use

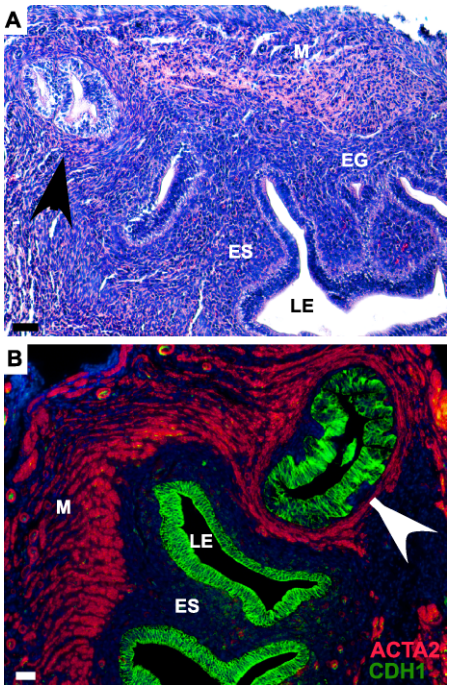


FIG. 6. **A**) H&E-stained section of mutant uterus showing hyperplasia and pseudostratification of epithelium of EGs. **B**) The longitudinal section of mutant uterus depicting the presence of EG in the myometrium stained with CDH1 (green) and ACTA2 (red) antibody, and counterstained with DAPI (blue). The arrowheads indicate ectopic endometrial tissue within the myometrium. LE, luminal epithelium; ES, endometrial stroma; EG, endometrial gland; M, myometrium. Bar = 50 μm.

findings suggest that tight regulation of the β-catenin signaling in ES and possibly myometrium is essential for the maintenance of normal EGs.

DISCUSSION

WNT signaling plays an important role in the development of the female reproductive tract [8–10, 20]. *Wnt4* mutant females have a defect in the development of Müllerian duct and show gonadal characteristics of males [20]. Similarly, deletion of *Wnt5a* leads to posteriorization of the female reproductive tract and causes a decrease in the thickness of myometrium [10]. The *Wnt7a* mutant males showed a defect in the regression of Müllerian duct, whereas females were infertile due to abnormal development of oviduct and uterus [8]. *Wnt7a* mutant uteri showed a lack of EGs and a decrease in the thickness of the myometrial layer of uterus as well [8]. Misregulated WNT signaling has been associated with the development of uterine tumors [7, 36]. The decrease in expression of secreted frizzled related proteins 4, an antagonist of WNT signaling, and concomitant increase in nuclear β-catenin is observed in the human ESS [7].

Consistent with a previous report [19], we observed that constitutive activation of β-catenin driven by the *Amhr2*-Cre induced ovarian anomalies in mice by 6 wk that were described as solid nests of disorganized cells. However, they showed that these mutant mice still had normal follicular and luteal structures and that a subset of older mutant mice developed ovarian tumors, which we also observed. Here we show that dysregulated WNT signaling in murine uterine mesenchymal cells via constitutively activated β-catenin leads to pleiotropic effects on uterine tumorigenesis as well. The unknown etiology of uterine mesenchymal tumors could be a primary reason for the limited progress toward development of therapeutics to prevent or manage leiomyomas. Currently, there are no mouse models that display uterine-specific mesenchymal tumors available for in-depth mechanistic analyses. In this study, we have shown that sustained activation of the WNT signaling pathway in ES and myometrium leads to the development of mesenchymal tumors in 100% of the mutant animals. In future studies we will use this mutant mouse model system to explore the molecular mechanisms and signaling pathways involved in leiomyoma and ESS tumorigenesis, with the goal of developing better treatment options.

For example, we have shown evidence that FRAP1 is affected by activated β-catenin in mutant mouse uteri. Uterine leiomyomas have also been observed in patients suffering from tuberous sclerosis and lymphangioleiomyomatosis, and there is evidence that half of human uterine leiomyomas show loss of tuberin, a protein product of tuberous sclerosis complex (TSC) 2 [37]. TSC 1/2 is the upstream regulator of FRAP1, and mutations in TSC1/2 lead to activation of FRAP1 signaling, which can lead to lymphangioleiomyomatosis and tuberous sclerosis in human patients [38]. A germline mutation in the TSC2 gene in rats leads to the development of uterine leiomyomas and leiomyosarcoma-like tumors in up to 65% of animals [28]. Additionally, activation and deletion of β-catenin in gastrointestinal stromal tumors both in vivo and in vitro have been shown to activate and down-regulate, respectively, the FRAP1 signaling pathway [39]. In other mouse model systems, mutations in *Pten*, a downstream inhibitor of the PI3 kinase pathway, have also been shown to correlate with more aggressive ovarian tumorigenesis when coupled with activated WNT signaling [34, 36, 40]. These findings suggest that WNT signaling and PI3 kinase signaling interactions could play an important role in the development of uterine tumors.

Alternatively, changes in uterine morphology during pregnancy and after parturition induce injury and repair mechanisms that stimulate tumorigenesis from stem/progenitor cells, which normally do not express constitutively activated β-catenin. This hypothesis is supported by the observation that the leiomyomas appeared near areas with prominent hemorrhaging and inflammation in multiparous mutant mice. The concept that uterine leiomyomas might be the end result of dysregulated fibrotic response and hypertrophic scarring has also been proposed by others [41]. These investigators suspected that uterine fibroids retained myofibroblasts, which are different from myometrial smooth muscle cells and which are also the extracellular matrix-depositing cells active in wound healing [23, 42–45]. Using their own published studies and those of others comparing leiomyoma and normal myometrium by microarray hybridizations [23, 42–45], they found, perhaps unsurprisingly, that the genes most consistently differentially regulated were those involved in extracellular matrix formation. The most consistently up-regulated gene was *TGFB3*, a member of the well-known TGFB cytokine family and a potent promoter of fibrosis [46]. They also showed electron microscopic evidence that the leiomyoma cells were indeed myofibroblasts and speculated that uterine fibroids were similar to keloids, in which repair of the injury extends beyond its original border. Furthermore, they made the interesting correlation that, as with keloids, leiomyomata uteri are disproportionally observed in African-American women, suggesting a genetic link between hypertrophic scarring and ethnicity.

We also observed ESS-like tumors in the $Amhr2^{tm3(cre)Bhr}/+$; $Ctnnb1^{tm1Mmt}/+$ mice with 100% penetrance. These ESS-like tumor lesions were positive for ESR1, vimentin, KIT, and HMGA2 and negative for E-cadherin (CDH1), ACTA2, PDGFRB (CD140B), and PECAM1. A similar immunohisto-

Downloaded From: https://bioone.org/journals/Biology-of-Reproduction on 28 Mar 2024
Terms of Use: https://bioone.org/terms-of-use

chemical expression pattern is also observed in human cases of ESS [47]. Additionally, genetic alternations in exon 3 of the β-catenin gene and subsequent stabilization of β-catenin in nucleus and/or cytoplasm are a common feature of various human tumors, including ovarian and uterine tumors [34, 36, 40]. Other human stromal tumors that express high levels of or have activating mutations in KIT are being relatively successfully treated with receptor tyrosine kinase inhibitors [48]. We suspect that human ESS might be amenable to similar therapies.

Recently, Jeong et al. [49] have shown that conditional activation of β-catenin with progesterone receptor (PGR)-driven Cre leads to the development of endometrial glandular hyperplasia. As PGR-Cre is expressed in all three compartments of the uterus (LE, ES, and myometrium), their study was unable to show whether the development of endometrial glandular hyperplasia is a direct result of activation of β-catenin in the epithelial cells or an indirect effect of activation in adjacent stromal cells. In the present study, we occasionally found both abnormal localization and hyperplasia of endometrial glands in the mutant uteri without constitutive activation of β-catenin in the epithelial cells, suggesting that dysregulated β-catenin signaling in stroma can also induce development of endometrial glandular hyperplasia. In summary, we have developed a mouse model to analyze the origin and progression of leiomyomas, ESSs, and adenomyosis and to devise novel treatment paradigms based on the molecular pathways we identify as targets for intervention.

ACKNOWLEDGMENTS

We would like to thank Drs. Patricia K. Donahoe, Henry L. Chang, and James K. Pru for their helpful suggestions and for reviewing this manuscript. We would like to thank Dr. Richard Behringer for providing us with the *Amhr2*$^{tm3(cre)Bhr}$ (*Amhr2*-Cre) mice.

REFERENCES

1. Cook JD, Walker CL. Treatment strategies for uterine leiomyoma: the role of hormonal modulation. Semin Reprod Med 2004; 22:105–111.
2. Walker CL, Stewart EA. Uterine fibroids: the elephant in the room. Science 2005; 308:1589–1592.
3. Mikels AJ, Nusse R. Wnts as ligands: processing, secretion and reception. Oncogene 2006; 25:7461–7468.
4. Polakis P. Wnt signaling and cancer. Genes Dev 2000; 14:1837–1851.
5. Ng TL, Gown AM, Barry TS, Cheang MC, Chan AK, Turbin DA, Hsu FD, West RB, Nielsen TO. Nuclear beta-catenin in mesenchymal tumors. Mod Pathol 2005; 18:68–74.
6. Jung CK, Jung JH, Lee A, Lee YS, Choi YJ, Yoon SK, Lee KY. Diagnostic use of nuclear beta-catenin expression for the assessment of endometrial stromal tumors. Mod Pathol 2008; 21:756–763.
7. Hrzenjak A, Tippl M, Kremser ML, Strohmeier B, Guelly C, Neumeister D, Lax S, Moinfar F, Tabrizi AD, Isadi-Moud N, Zatloukal K, Denk H. Inverse correlation of secreted frizzled-related protein 4 and beta-catenin expression in endometrial stromal sarcomas. J Pathol 2004; 204:19–27.
8. Parr BA, McMahon AP. Sexually dimorphic development of the mammalian reproductive tract requires Wnt-7a. Nature 1998; 395:707–710.
9. Miller C, Sassoon DA. Wnt-7a maintains appropriate uterine patterning during the development of the mouse female reproductive tract. Development 1998; 125:3201–3211.
10. Mericskay M, Kitajewski J, Sassoon D. Wnt5a is required for proper epithelial-mesenchymal interactions in the uterus. Development 2004; 131:2061–2072.
11. Xie H, Tranguch S, Jia X, Zhang H, Das SK, Dey SK, Kuo CJ, Wang H. Inactivation of nuclear Wnt-beta-catenin signaling limits blastocyst competency for implantation. Development 2008; 135:717–727.
12. Herington JL, Bi J, Martin JD, Bany BM. Beta-catenin (CTNNB1) in the mouse uterus during decidualization and the potential role of two pathways in regulating its degradation. J Histochem Cytochem 2007; 55:963–974.
13. Mohamed OA, Jonnaert M, Labelle-Dumais C, Kuroda K, Clarke HJ, Dufort D. Uterine Wnt/beta-catenin signaling is required for implantation. Proc Natl Acad Sci U S A 2005; 102:8579–8584.
14. Jamin SP, Arango NA, Mishina Y, Behringer RR. Genetic studies of MIS signalling in sexual development. Novartis Found Symp 2002; 244:157–164; discussion 164–158, 203–156, 253–157.
15. Arango NA, Szotek PP, Manganaro TF, Oliva E, Donahoe PK, Teixeira J. Conditional deletion of beta-catenin in the mesenchyme of the developing mouse uterus results in a switch to adipogenesis in the myometrium. Dev Biol 2005; 288:276–283.
16. Harada N, Tamai Y, Ishikawa T, Sauer B, Takaku K, Oshima M, Taketo MM. Intestinal polyposis in mice with a dominant stable mutation of the beta-catenin gene. EMBO J 1999; 18:5931–5942.
17. Jamin SP, Arango NA, Mishina Y, Hanks MC, Behringer RR. Requirement of Bmpr1a for Mullerian duct regression during male sexual development. Nat Genet 2002; 32:408–410.
18. Teixeira J, He WW, Shah PC, Morikawa N, Lee MM, Catlin EA, Hudson PL, Wing J, Maclaughlin DT, Donahoe PK. Developmental expression of a candidate mullerian inhibiting substance type II receptor. Endocrinology 1996; 137:160–165.
19. Boerboom D, Paquet M, Hsieh M, Liu J, Jamin SP, Behringer RR, Sirois J, Taketo MM, Richards JS. Misregulated Wnt/beta-catenin signaling leads to ovarian granulosa cell tumor development. Cancer Res 2005; 65: 9206–9215.
20. Vainio S, Heikkila M, Kispert A, Chin N, McMahon AP. Female development in mammals is regulated by Wnt-4 signalling. Nature 1999; 397:405–409.
21. Lamminen S, Rantala I, Helin H, Rorarius M, Tuimala R. Proliferative activity of human uterine leiomyoma cells as measured by automatic image analysis. Gynecol Obstet Invest 1992; 34:111–114.
22. Arici A, Sozen I. Transforming growth factor-beta3 is expressed at high levels in leiomyoma where it stimulates fibronectin expression and cell proliferation. Fertil Steril 2000; 73:1006–1011.
23. Catherino WH, Leppert PC, Stenmark MH, Payson M, Potlog-Nahari C, Nieman LK, Segars JH. Reduced dermatopontin expression is a molecular link between uterine leiomyomas and keloids. Genes Chromosomes Cancer 2004; 40:204–217.
24. Chegini N, Ma C, Tang XM, Williams RS. Effects of GnRH analogues, 'add-back' steroid therapy, antiestrogen and antiprogestins on leiomyoma and myometrial smooth muscle cell growth and transforming growth factor-beta expression. Mol Hum Reprod 2002; 8:1071–1078.
25. Dou Q, Zhao Y, Tarnuzzer RW, Rong H, Williams RS, Schultz GS, Chegini N. Suppression of transforming growth factor-beta (TGF beta) and TGF beta receptor messenger ribonucleic acid and protein expression in leiomyomata in women receiving gonadotropin-releasing hormone agonist therapy. J Clin Endocrinol Metab 1996; 81:3222–3230.
26. Lee BS, Nowak RA. Human leiomyoma smooth muscle cells show increased expression of transforming growth factor-beta 3 (TGF beta 3) and altered responses to the antiproliferative effects of TGF beta. J Clin Endocrinol Metab 2001; 86:913–920.
27. Wullschleger S, Loewith R, Hall MN. TOR signaling in growth and metabolism. Cell 2006; 124:471–484.
28. Everitt JI, Wolf DC, Howe SR, Goldsworthy TL, Walker C. Rodent model of reproductive tract leiomyomata. Clinical and pathological features. Am J Pathol 1995; 146:1556–1567.
29. Brody JR, Cunha GR. Histologic, morphometric, and immunocytochemical analysis of myometrial development in rats and mice, I: normal development. Am J Anat 1989; 186:1–20.
30. Rushing RS, Shajahan S, Chendil D, Wilder JL, Pulliam J, Lee EY, Ueland FR, van Nagell JR, Ahmed MM, Lele SM. Uterine sarcomas express KIT protein but lack mutation(s) in exon 11 or 17 of KIT. Gynecol Oncol 2003; 91:9–14.
31. Erdogan G, Bassorgun CI, Pestereli HE, Simsek T, Karaveli S. KIT protein expression in uterine and ovarian mesenchymal tumours. APMIS 2007; 115:204–209.
32. D'Armiento J, Imai K, Schiltz J, Kolesnekova N, Sternberg D, Benson K, Pardo A, Selman M, Smolarek T, Vundavalli M, Sonnet J, Szabolcs M, Chada K. Identification of the benign mesenchymal tumor gene HMGA2 in lymphangiomyomatosis. Cancer Res 2007; 67:1902–1909.
33. Zaidi MR, Okada Y, Chada KK. Misexpression of full-length HMGA2 induces benign mesenchymal tumors in mice. Cancer Res 2006; 66:7453–7459.
34. Iwao K, Nakamori S, Kameyama M, Imaoka S, Kinoshita M, Fukui T, Ishiguro S, Nakamura Y, Miyoshi Y. Activation of the beta-catenin gene by interstitial deletions involving exon 3 in primary colorectal carcinomas without adenomatous polyposis coli mutations. Cancer Res 1998; 58: 1021–1026.
35. Miyoshi Y, Iwao K, Nagasawa Y, Aihara T, Sasaki Y, Imaoka S, Murata

Downloaded From: https://bioone.org/journals/Biology-of-Reproduction on 28 Mar 2024
Terms of Use: https://bioone.org/terms-of-use

M, Shimano T, Nakamura Y. Activation of the beta-catenin gene in primary hepatocellular carcinomas by somatic alterations involving exon 3. Cancer Res 1998; 58:2524–2527.
36. Fukuchi T, Sakamoto M, Tsuda H, Maruyama K, Nozawa S, Hirohashi S. Beta-catenin mutation in carcinoma of the uterine endometrium. Cancer Res 1998; 58:3526–3528.
37. Wei J, Chiriboga L, Mizuguchi M, Yee H, Mittal K. Expression profile of tuberin and some potential tumorigenic factors in 60 patients with uterine leiomyomata. Mod Pathol 2005; 18:179–188.
38. Sarbassov DD, Ali SM, Sabatini DM. Growing roles for the FRAP1 pathway. Curr Opin Cell Biol 2005; 17:596–603.
39. Fujishita T, Aoki K, Lane HA, Aoki M, Taketo MM. Inhibition of the FRAP1C1 pathway suppresses intestinal polyp formation and reduces mortality in ApcDelta716 mice. Proc Natl Acad Sci U S A 2008; 105: 13544–13549.
40. Wu R, Hendrix-Lucas N, Kuick R, Zhai Y, Schwartz DR, Akyol A, Hanash S, Misek DE, Katabuchi H, Williams BO, Fearon ER, Cho KR. Mouse model of human ovarian endometrioid adenocarcinoma based on somatic defects in the Wnt/beta-catenin and PI3K/Pten signaling pathways. Cancer Cell 2007; 11:321–333.
41. Leppert PC, Catherino WH, Segars JH. A new hypothesis about the origin of uterine fibroids based on gene expression profiling with microarrays. Am J Obstet Gynecol 2006; 195:415–420.
42. Tomasek JJ, Gabbiani G, Hinz B, Chaponnier C, Brown RA. Myofibroblasts and mechano-regulation of connective tissue remodelling. Nat Rev Mol Cell Biol 2002; 3:349–363.
43. Hoffman PJ, Milliken DB, Gregg LC, Davis RR, Gregg JP. Molecular characterization of uterine fibroids and its implication for underlying mechanisms of pathogenesis. Fertil Steril 2004; 82:639–649.
44. Luo X, Ding L, Xu J, Chegini N. Gene expression profiling of leiomyoma and myometrial smooth muscle cells in response to transforming growth factor-beta. Endocrinology 2005; 146:1097–1118.
45. Zhao Y, Wen Y, Polan ML, Qiao J, Chen BH. Increased expression of latent TGF-beta binding protein-1 and fibrillin-1 in human uterine leiomyomata. Mol Hum Reprod 2007; 13:343–349.
46. Armour A, Scott PG, Tredget EE. Cellular and molecular pathology of HTS: basis for treatment. Wound Repair Regen 2007; 15(suppl 1):S6–S17.
47. Moinfar F, Azodi M, Tavassoli FA. Uterine sarcomas. Pathology 2007; 39:55–71.
48. Rubin BP, Heinrich MC, Corless CL. Gastrointestinal stromal tumour. Lancet 2007; 369:1731–1741.
49. Jeong JW, Lee HS, Franco HL, Broaddus RR, Taketo MM, Tsai SY, Lydon JP, Demayo FJ. Beta-catenin mediates glandular formation and dysregulation of beta-catenin induces hyperplasia formation in the murine uterus. Oncogene 2009; 28:31–40.

Downloaded From: https://bioone.org/journals/Biology-of-Reproduction on 28 Mar 2024
Terms of Use: https://bioone.org/terms-of-use